Computational study of ridge states in GaAs nanopillars

Ted H. Yu[1,2,a)] and Christian Ratsch[2]
[1]*Department of Chemical Engineering, California State University, Long Beach, California 90840, USA*
[2]*Department of Mathematics and Institute of Pure and Applied Mathematics, University of California, Los Angeles, California 90095, USA*

(Received 8 May 2015; accepted 23 July 2015; published online 6 August 2015)

Semiconductor nanopillars have unique geometries that make them very promising materials for a variety of devices. In order to improve their performance, we need to understand how they are affected by ridge states that lie on the six corners of the nanopillar hexagon. Although the GaAs nanopillars are primarily zinc blende (ABC), stacking faults of wurtzite (AB) stacking occur. We use density-functional theory to study stacking faults using one-dimensional periodic geometries that have a combination of zinc blende and wurtzite stacking. In contrast to perfect zinc blende nanopillars, energetically favorable midgap ridge states created by stacking faults are found in these geometries using density-functional theory. The calculated band diagrams and densities of state help us to understand how these midgap states lead to a reduced mobility and carrier localization. We also study how sulfur passivation affects and potentially improves the performance by modifying the ridges. © *2015 AIP Publishing LLC*. [http://dx.doi.org/10.1063/1.4927923]

I. INTRODUCTION

State-of-the-art semiconductor nanopillars are an exciting new topic, due to their unique properties that can be used in a number of microelectronic applications.[1–14] Nanopillars can be grown into microarrays that can maximize surface to volume ratio, ideal for photo-voltaic applications.[2,7,8] In this paper, we focus on GaAs nanopillars. One of the issues with growing GaAs nanopillars is the existence of stacking faults[1,15–17] that occur during growth. Both ABC and AB stacking exist in the nanopillars, even though the bulk ABC (zinc blende) stacking is energetically favored versus wurtzite (ABAB) stacking by 0.03 eV per GaAs.[18] Although stacking faults can be controlled to a certain extent, it is difficult with current technology to grow catalyst-free nanopillars without stacking faults, although there are a number of publications on gold-assisted vapour-liquid-solid grown nanowires that are entirely twin-free.[11,12]

There are a number of theoretical studies that have looked at GaAs nanopillars. Cahangirov and co-worker[18] have studied zinc blende and wurtzite nanopillars of different diameters and have found that the energy of formation, E_{form}, decreases with larger nanopillar diameter. Although the wurtzite nanopillars did not have any significant midgap states, the zinc blende nanopillars typically have a number of midgap ridge states that could be removed by adding pseudo-hydrogen atoms (of 0.75 or 1.25 electrons) to the ridges formed by the corners of the nanopillar hexagon. Rosini and co-worker[19] have found that these ridge states can be removed by ridge reconstruction for certain stackings/orientations, where the removal of Ga and As atoms along the ridges restores the bulk GaAs band structure. Midgap states lead to poor carrier mobility and localization which are crucial for device applications. Kratzer and co-workers[20] have studied the effect of the edge dangling bonds to determine whether a wurtzite or zinc blende layer is favored near the edges. These studies have employed geometries of about 50–400 atoms per layer that are periodic only in the perpendicular direction. Larger radius nanopillars, closer to the size of experiments, are difficult to study due to the atom limit of density-functional theory (DFT). In all of these studies, the wurtzite formation energy of these small nanopillars were found to be lower than formation energy for zinc blende due to the lower wurtzite surface energy found in small radius nanopillars. This is contrary to the infinite radius nanopillar where the zinc blende is more favorable. Edge effects allow wurtzite stacking faults to occur even though they are not energetically favorable in the bulk.

To study stacking faults theoretically, we employ geometries similar to those aforementioned. Instead of the $(AB)_n$ and $(ABC)_n$ stacking for wurtzite and zinc blende, our challenge is to simulate a stacking fault of similarly sized pillars. A stacking fault occurs when there is a twin in the zinc blende stacking such as described below. We can approximate this by using a $(ABCB)_n$ or polytype stacking as shown in Figure 1 where we highlight the stacking fault of A-B-C-B-A.

We will use these models to study how ridge states can be removed through chemical sulfur passivation. Recently, it was shown that sulfur passivation (which is a common method to passivate III–V semiconductors[10,21]) can improve GaAs nanopillar solar energy conversion.[2] Although there are theoretical studies on the effect of sulfur passivation on planar GaAs surfaces,[22–24] the study of sulfur passivation for GaAs nanopillars is lacking. We consider GaAs nanopillar consisting of (111) and (110) surfaces, because they are predominant in catalyst-free nanopillar growth where stacking faults play a large role.[15] We note that other facets such as the (112) surface[11] also appear under different conditions. Our previous paper[23] demonstrated that the surface states can be caused by As or Ga deficiencies on the surface, but it

a)Electronic mail: ted.yu@csulb.edu

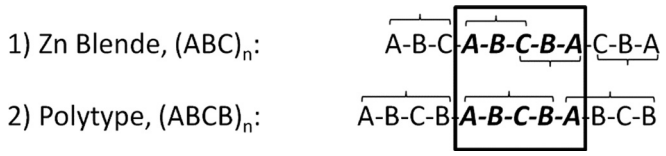

FIG. 1. Illustration of the polytype, $(ABCB)_n$, as a means to simulate a wurtzite twin, stacking fault occurring in a zinc blende stacking, $(ABCB)_n$.

was found that these deficiencies are more difficult to create on the (111) and (110) surfaces than the (100) surface. Unlike the GaAs (100) surface, the (111) and (110) surfaces of a GaAs nanopillar are probably defect free, as there are no reports of sulfur passivation device enhancement effects on the GaAs (110) and (111) surfaces in the same papers[25,26] that showed native oxides were removed through passivation. In addition, our previous work[23] showed that the energy to create a defect in the GaAs (111B) and (110) surfaces is much more energetically difficult than in the GaAs (100) surface. The defect energy for the (100) surface was 0.84 eV, while that for (110) surface was 1.77 eV and that for the (111B) surface was 1.45 eV at intermediate chemical potentials. Our work showed a model where the surface state created by the defect on the GaAs (100) can be removed by sulfur passivation. However, we do not believe this is the mechanism in which sulfur passivation removes midgap states in GaAs nanopillars, as the energy to form defects on the (111) and (110) surfaces are too high.

II. METHOD

We use the FHI-AIMS[27] code for our DFT calculations. It is an all-electron code that uses atom centered numeric orbitals as a basis set. For these calculations, DFT with the Perdew-Burke-Ernzerhof (PBE)[28] approximation of the generalized gradient approximation (GGA) exchange-correlation functional and with accurate van der Waals (VdW) corrections[29] is used. We use the predefined light basis setting, which has radial s, p, and d characters with an overall cutoff radius of 5 Å and a Hartree potential expansion up to $l = 4$. Using this setting with PBE + VdW, we obtained GaAs lattice parameters of 2.855 Å, a 1.1% deviation from the experimental lattice parameter of 2.825 Å. For the nanopillars which are periodic in the z-direction, only atoms within the center hexagon of 2.35 Å are fixed during geometry relaxation. Using the optimized lattice parameter, our nanopillars were found to have band gaps ranging from 0.92 to 1.22 eV. The bulk band gap of 0.34 eV is underestimated from the experimental value of 1.4 eV, as it has been shown previously that PBE underestimates the band gap. The main purpose of this calculation is to address whether a nanopillar is metallic or semiconducting and using the computationally more efficient PBE functional qualitatively addresses this important issue. The size of the super cell in the x and y directions is 50 Å, compared to a maximum nanopillar diameter of 16.68 Å, in order to minimize the interaction between the sides of the nanopillars. The periodicities in the z-direction are: 13.28 Å for polytype and 9.96 Å for zinc blende. The k-points are $1 \times 1 \times 3$ and $1 \times 1 \times 4$, respectively, and we tested that this was sufficient to get accurate results.

III. RESULTS AND DISCUSSION

There are two hexagonal sizes studied: the smaller hexagon has a radius of 6.49 Å and the larger hexagon has a radius of 8.34 Å. Unlike previous studies which studied both (112) and (110) facets of nanopillars,[18–20] we focus only on nanopillars with (110) type facets as these are experimentally observed.[20] To study the effects of the stacking faults, we first need to establish the model for the zinc blende nanopillar without stacking faults to understand what changes when stacking faults are introduced. Then, we will look at a polytype or $(ABCB)_n$ stacking. For the polytype, 50% of the layers are considered wurtzite, because any particular layer has identical layer neighbors both above and below (either A or B). The other 50% of the layers are considered zinc blende, because the layers above and below any particular layer are always different. This makes the stacking 50% wurtzite and 50% zinc blende.

The layers A, B, and C of the smaller (6.49 Å) hexagon are shown in Figure 2 with three stacking sequences: one zinc blende (zinc blende1) and two polytypes (polytype1 and polytype2). Similarly, the layers of the larger (8.53 Å) nanopillars are shown in Figure 3 with zinc blende2, polytype3, and polytype4. The different polytype cases represent different terminations. They are both of the form ABCB, and would be identical if the nanopillars were extended to infinity along the x and y axes. They represent differences in the way the nanopillars terminate at the corners, which form different unique ridges identified as P1, P2, and P3.

A. Nanopillars without stacking faults, zinc blende $(ABC)_n$

We first model fault-free nanopillars which are of $(ABC)_n$ periodicity. We model two radii cases, periodic in

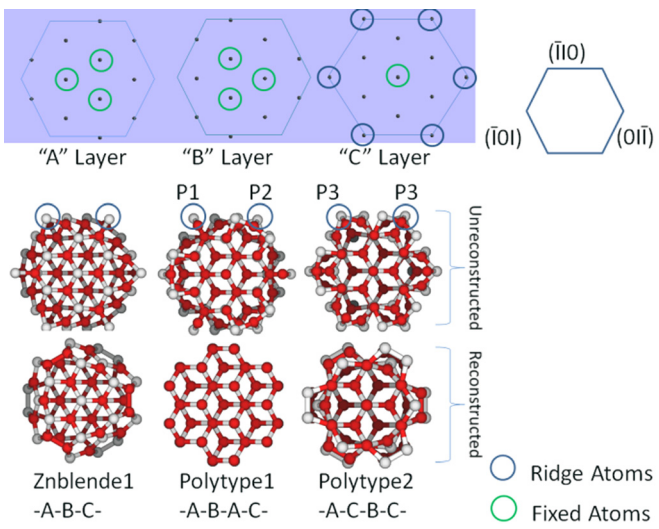

FIG. 2. Top panel: The atomic location of the 6.49 Å radius nanopillar perpendicular to the [111] z-direction. An "A" stack contains 24 atoms (or 12 GaAs), a "B" stack contains 24 atoms, and a "C" stack contains 26 atoms. Bottom panel: The relaxed structures of the different stacking geometries before and after ridge reconstruction. Ga and As atoms are red and white, respectively. The zinc blende and polytype ridge atoms are highlighted in dark blue circles, with the polytype ridges labelled P1, P2, and P3. The zinc blende ridges are also circled. The bonding of the ridges is described in Table II.

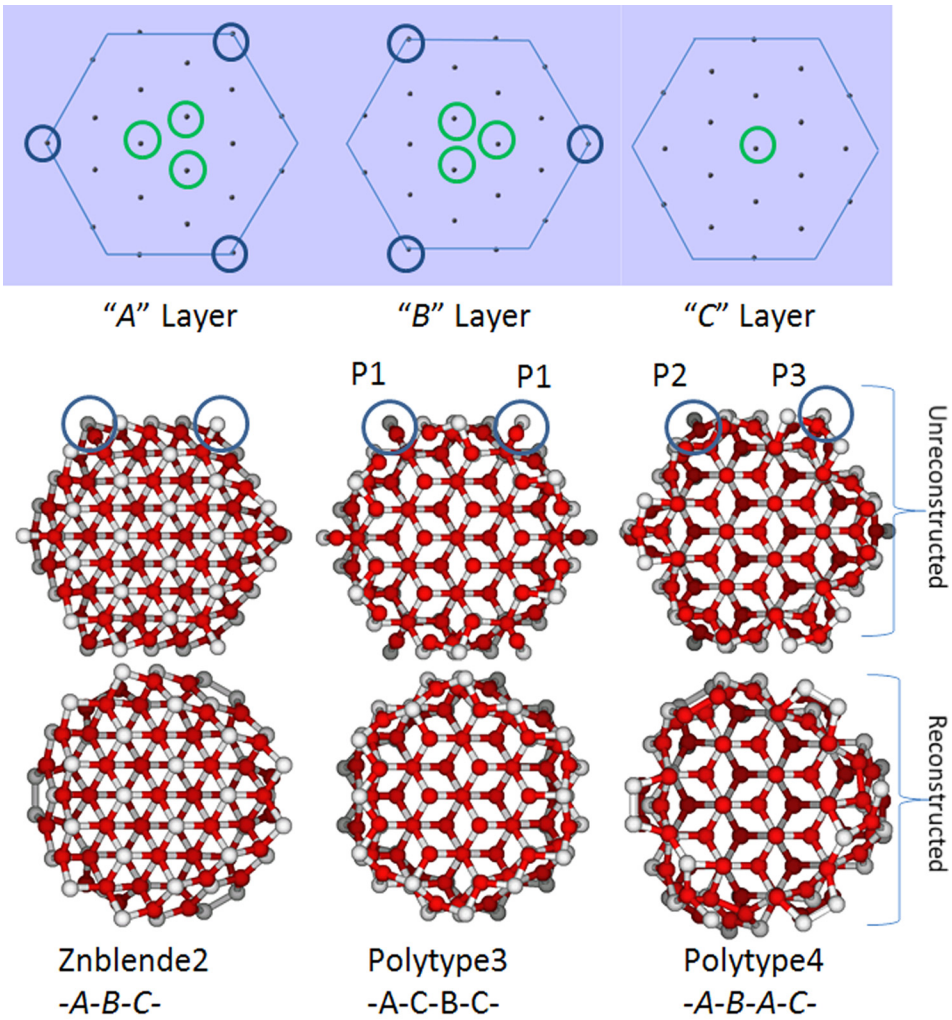

FIG. 3. Top panel: The atomic location of the 8.53 Å radius nanopillar along perpendicular to the [111] z-direction. An "A" stack contains 42 atoms, a "B" stack contains 42 atoms, and a "C" stack contains 38 atoms. Bottom panel: The relaxed structures of the different stacking geometries before and after ridge reconstruction, Ga (Red) and As (White) atoms. The zinc blende and polytype ridge atoms are highlighted in dark blue circles, with the polytype ridges labelled P1, P2, and P3. The zinc blende ridges are also circled, unlabelled. The bonding of the ridges is described in Table II.

the [111] direction and the side walls are (110), (101), and (011) surfaces. To measure stability, we assess the formation energy, E_F, as

$$E_F = \frac{E_{nanopilar}}{\#GaAs\,pairs} - \mu_{GaAs}, \tag{1}$$

where μ_{GaAs} is the total energy of the zinc blende primitive cell. The energy and band gaps of the nanopillars are compared to previous calculations[19] that used DFT with the Local Density Approximation (LDA). The results are shown in Figure 4. The unreconstructed cases are nanopillars that include the ridge atoms as shown in Figures 2 and 3 marked in dark blue circles. These ridge atoms are removed for the reconstructed cases.

From the results in Table I and Figure 4, we can see that both the band gap and energy of formation is radius dependent. They both approach the bulk values as the radius

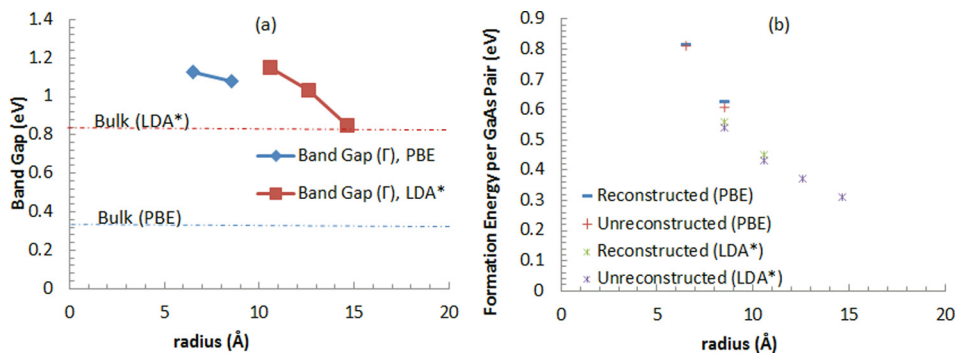

FIG. 4. Zinc blende stacking nanopillar band gap (a) and formation energy (b) as a function of the radius. (a) The calculated direct band gaps of reconstructed nanopillars are shown for this work (PBE) and a previous work (LDA).[19] The dashed line represents the calculated band gap for bulk zinc blende. (b) The formation energy per GaAs pair is calculated in Equation (1). The results of this work are labelled as (PBE) and compared with previous results that are labeled (LDA).[19] The reconstructed nanopillars are semiconductors and unreconstructed nanopillars are metals (see also Table I). The reconstructed nanopillars are energetically favored $(ABC)_n$ stacking.

TABLE I. band gap and energy data for different nanopillar stacking: zinc blende and polytype. The band gap is shown with the reconstructed band gap in parenthesis. The nanopillar atomic formula is shown with the reconstructed atomic formula in parenthesis. The energy of formation per GaAs is calculated in Equation (1). This number is repeated for the reconstructed case. The difference in unreconstructed vs. reconstructed is shown, with Zinc blende1, Zinc blende2, and Polytype3 favoring reconstruction.

	Band gap (PBE) unreconstructed (reconstructed) in eV	Atomic formula: unreconstructed (reconstructed)	Unreconstructed $E_{formation}$/GaAs (reconstructed) in eV	Difference in eV
Zinc blende1 (-A-B-C-)	0.01 (1.13)	$Ga_{37}As_{37}$ ($Ga_{31}As_{31}$)	0.816 (0.807)	−0.009
Zinc blende2 *(-A-B-C-)*	0.01 (1.08)	$Ga_{61}As_{61}$ ($Ga_{55}As_{55}$)	0.626 (0.603)	−0.023
Polytype1 (-A-B-A-C-)	0.77 (0.92)	$Ga_{49}As_{49}$ ($Ga_{43}As_{43}$)	0.711 (0.768)	+0.056
Polytype2 (-A-C-B-C-)	0.02 (1.03)	$Ga_{50}As_{50}$ ($Ga_{37}As_{37}$)	0.875 (0.904)	+0.029
Polytype3 *(-A-C-B-C-)*	0.98 (1.02)	$Ga_{80}As_{80}$ ($Ga_{74}As_{74}$)	0.593 (0.554)	−0.038
Polytype4 *(-A-B-A-C-)*	0.05 (1.22)	$Ga_{82}As_{82}$ ($Ga_{73}As_{73}$)	0.593 (0.622)	+0.029

increases. For all radii, we find that the formation energy is lower for reconstructed cases than for unreconstructed cases for pure zinc blende nanopillars. It is energetically favorable for nanopillars of zinc blende stacking to reconstruct. This reconstruction restores the band gap and changes the nanopillar from a metal to a semiconductor.

B. Nanopillars with stacking faults, polytype $(ABCB)_n$

To emulate a stacking fault, four-layered polytype stacking nanopillars are studied. The simplest polytype stacking has a periodic stacking order of ABCB. Because of the differences in termination of the nanopillars, there are two types: ABAC and ACBC; note that BABC is identical to ABAC (A and B layers are mirror images of each other). Polytype1 and polytype4 are ABAC, while polytype2 and polytype3 are ACBC. The ridge atoms described in Figures 1 and 2 are removed to study ridge reconstruction. Figure 5 shows how the ridge reconstruction affects the energy of formation as calculated from Equation (1).

We see from Figure 5 that polytype1, polytype2, and polytype4 are energetically unfavorable to undergo ridge reconstruction. Since ridge reconstruction changes the zinc blende nanopillars (without stacking faults) from a metal to a semiconductor, we examine the direct band gaps of unreconstructed polytype1, 2, and 4. We find that polytypes 2 and 4 are metals (Table I). Since polytype stacking emulates a stacking fault occurring every four layers, this result shows that these metal states appear when stacking faults appear in the large frequency described by our model, although the results also suggest that these states may appear in smaller frequency stacking faults. Each polytype stacking can have two different types of ridges, where three of the six ridges are one type, while the other three have another ridge type. We identify three ridges for the different polytype cases, P1, P2, and P3, as shown in Figures 2 and 3, detailed in Table II. We see that only polytype3 is energetically favorable to reconstruct, and it contains only P1 ridges. Examining P2 ridges, we see that all of the cases with P2 ridges (polytype1 and polytype2) are not energetically favorable to reconstruct. Finally, the P3 ridges are found in polytype2 and polytype4, which are not energetically favorable to reconstruct. Using this analysis, we conclude that P2 and P3 ridges are not favorable to reconstruct.

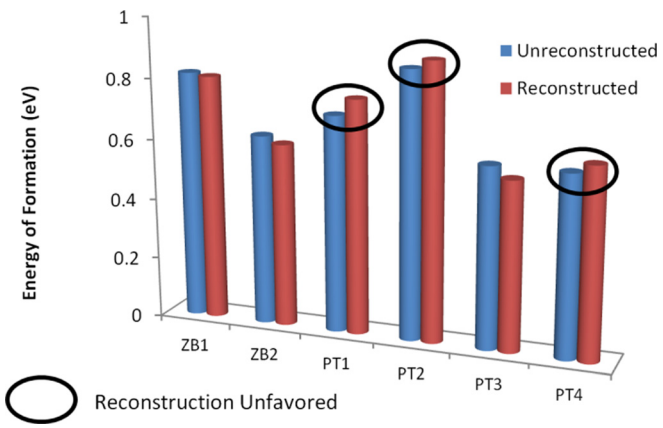

FIG. 5. Zinc blende (ZB) and polytype (PT) stacking nanopillar formation energies. The formation energy per GaAs pair calculated in Equation (1). Ridge reconstruction was calculated to be energetically unfavorable for PT1, PT2, and PT4.

From Table I, we see that polytype1 and polytype3 are semiconducting even before reconstruction. On the other hand, polytype2 and polytype4 are metallic. Since P1 and P2 ridges are both present in polytype1, which is semiconducting, we conclude that both P1 and P2 ridges do not contain metallic states. Since P3 ridges are present in polytype2 and polytype4, this data suggests that the P3 ridges can cause the metallic states in nanopillars. To see if P3 ridges cause metallic states at larger separation distances, a model larger than four layers is required to see if an isolated stacking fault leads to energetically favorable localized electronic states in the band gap. Table II summarizes our conclusions of the three polytype ridge types.

C. The role of sulfur passivation

To investigate how sulfur passivates a polytype GaAs nanopillar, we investigate where it prefers to bond to the two ridge types where reconstruction is not favored, P2 and P3. To simulate the reaction of sulfur on P2 and P3 ridges, we use unreconstructed polytype1 and polytype2 (Figure 1) as our starting point. For polytype1, because the P1 ridges are favored for reconstruction, while the P2 ridges are not, we removed the P1 ridge as the starting point. Then, we replace

TABLE II. Description of nanopillar ridges: The ridge atom density describes the percentage of atoms that lie in the corner of the nanopillar. For the smaller radius example, polytype2 contains ACBC stacking. Ridge atoms only occurs in C layers and not in A or B layers, which leads to a density of 50%. Polytype1 contains ABAC stacking, which leads to a density of 25% for P1 and P2. There are either two or three Ga or As neighbor atoms. The P2 and P3 ridges are shown in Figure 5.

		Types of atoms on ridge					
Ridge type	Ridge atom density	2-fold Ga	2-fold As	3-fold Ga	3-fold As	Metallic	Energetically favorable to reconstruct
P1	25%	X	X			No	Yes
P2	25%			X	X	No	No
P3	50%	X	X	X	X	Yes	No

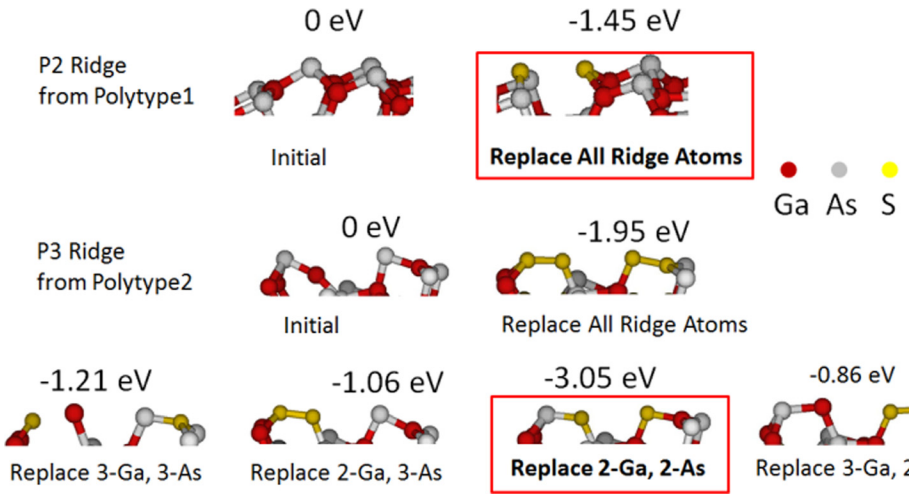

FIG. 6. Schematic representation of different sulfur passivation scenarios of P2 and P3 ridges. For P3, the formation energies show that two sulfurs replacing just the 2-fold Ga and 2-fold As is the energetically most favorable substitution.

ridge GaAs with S at different positions to calculate the sulfur substitution energy, E_{SS}, as shown in Figure 6,

$$E_{SS} = \frac{E_{nanopillar-S} + N(\mu_{GaAs}) - E_{nanopillar} - 2N(\mu_S)}{\#\ of\ ridges\ substituted}, \quad (2)$$

where $E_{nanopillar}$ is the energy of nanopillars before sulfur substitution, $E_{nanopillar\text{-}S}$ is the energy of nanopillars after sulfur substitution, N is the number of GaAs substituted on the ridges, μ_{GaAs} and μ_S are the bulk energy of GaAs and sulfur, respectively. The number of ridges substituted is three and six, respectively, for polytype1 and polytype2. For the P2 ridge, there was only one possible substitution of GaAs for two sulfurs, and that energy was calculated to be -1.45 eV in favor of substitution. For the P3 ridge, there are five possible substitution configurations. The most stable was found to have a substitution energy of -3.05 eV. All the configurations are shown in Figure 6.

From Figure 6, we see that sulfur substitution is favorable on the ridges P2 and P3. Since the P2 ridge is already semiconducting, sulfur substitution did not affect its properties. The PBE direct band gap changed from 0.92 eV to 0.85 eV. For the P3 ridge, replacing GaAs by two sulfurs, it was found that replacing the As(2-fold) and Ga(2-fold) is most favorable with an energy of -3.05 eV per ridge. This sulfur substitution changed the metallic P3 ridge to semiconducting. In Figure 7, we find that midgap states at the Fermi level are removed in this configuration and a partial direct bandgap of 0.70 eV is restored with an indirect band gap of 0.94 eV. Evaluating the band structure, we see that the entire band structure gets shifted when S replaces GaAs so that the Fermi energy moved from the bottom of the conduction band of the non-passivated case to the middle of the band gap of the sulfur-passivated case. Figure 7 shows the band structure and density of states of the metallic to semiconducting transition during sulfur passivation of P3 ridges.

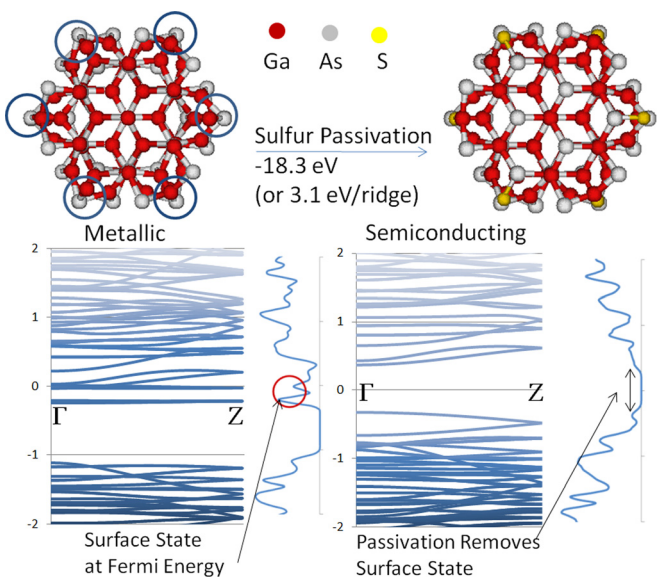

FIG. 7. Geometry and density of State for a polytype2 nanopillar before and after sulfur passivation of P3 ridges. Sulfur passivation is shown to remove midgap states restoring a direct band gap, $E_{g,\Gamma} = 0.70$ eV, indirect band gap, $E_{g,Z} = 0.94$ eV. The zero represents the Fermi energy.

IV. CONCLUSION

DFT was used to model nanopillars with and without stacking faults. The zinc blende nanopillars are stacking fault free. Their ridge metallic states were found to be removed when the ridges reconstruct in agreement with previous studies. The stacking faults were modeled with a four-layer polytype stacking which emulates stacking faults occurring with large frequency. Three ridges were identified, and two of them were found to be energetically unfavorable to reconstruct. The P3 ridge is one of them, and it has metallic states that cross the Fermi energy. Removal of metallic states leads to increased mobility and less carrier localization, both crucial for device applications. We found an energetically favorable configuration for P3 ridges when sulfur substitutes GaAs during sulfur passivation. The band structure and density of state show that sulfur passivation changes the ridge from metallic to semiconducting. Since sulfur passivation has been found to improve the performance of GaAs nanopillars, our mechanism details how sulfur may react with GaAs nanopillars during chemical passivation when stacking faults are isolated, while our conclusion only holds when stacking faults occur at a frequency of one in every four stacks.

ACKNOWLEDGMENTS

This work was funded by the National Science Foundation under Grant No. DMR-1125931. We would like to thank participants of the IPAM program on "Materials Defects: Mathematics, Computation, and Engineering" for fruitful discussions, especially Peter Kratzer and Joshua Shapiro. We appreciate the FHI-AIMS team for help with the FHI-AIMS code. We also thank our experimental collaborators for their experience and insight: Liang Yan, Wei You, Giacomo Mariani, Ramesh Laghumavarapu, and Diana Huffaker.

[1]A. Lin, J. N. Shapiro, P. N. Senanayake, A. C. Scofield, P. S. Wong, B. L. Liang, and D. L. Huffaker, Nanotechnology **23**, 105701 (2012).
[2]G. Mariani, R. B. Laghumavarapu, B. T. de Villers, J. Shapiro, P. Senanayake, A. Lin, B. J. Schwartz, and D. L. Huffaker, Appl. Phys. Lett. **97**(1), 013107 (2010).
[3]P. Senanayake, C. H. Hung, A. Farrel, D. A. Ramirez, J. Shapiro, C. K. Li, Y. R. Wu, M. M. Hayat, and D. L. Huffaker, Nano Lett. **12**, 6448–6452 (2012).
[4]A. C. Scofield, Se.-H. Kim, J. Shapiro, A. Lin, B. Liang, A. Scherer, and D. L. Huffaker, Nano Lett. **11**, 5387 (2011).
[5]K. Tomioka, M. Yoshimura, and T. Fukui, Nature **488**, 189–192 (2012).
[6]T. Tanaka, K. Tomioka, S. Hara, J. Motohisa, E. Sano, and T. Fukui, Appl. Phys. Express **3**, 025003 (2010).
[7]G. Mariani, P. S. Wong, A. M. Katzenmeyer, F. Leonard, J. Shapiro, and D. L. Huffaker, Nano Lett. **11**(6), 2490–2494 (2011).
[8]G. Mariani, A. C. Scofield, C. H. Hung, and D. L. Huffaker, Nat. Commun. **4**, 1497 (2013).
[9]S. Breuer, M. Hilse, A. Trampert, L. Geelhaar, and H. Riechert, Phys. Rev. B **82**(7), 075406 (2010).
[10]M. H. Sun, H. J. Joyce, Q. Gao, H. H. Tan, C. Jagadish, and C. Z. Ning, Nano Lett. **12**(7), 3378–3384 (2012).
[11]H. Shtrikman, R. Popovitz-Biro, A. Kretinin, and M. Heiblum, Nano Lett. **9**(4), 215–219 (2009).
[12]H. J. Joyce, Q. Gao, H. H. Tan, C. Jagadish, Y. Kim, X. Zhang, Y. Guo, and J. Zou, Nano Lett. **7**(4), 921 (2007).
[13]M. Yao, N. Huang, S. Cong, C. Y. Chi, M. A. Seyedi, Y. T. Lin, Y. Cao, M. L. Povinelli, P. D. Dapkus, and C. Zhou, Nano Lett. **14**(6), 3293–3303 (2014).
[14]P. Schroth, M. Kohl, J. W. Hornung, E. Dimakis, C. Somaschini, L. Geelhaar, A. Biermanns, S. Bauer, S. Lazarev, U. Pietsch, and T. Baumbach, Phys. Rev. Lett. **114**, 055504 (2015).
[15]J. N. Shapiro, A. Lin, C. Ratsch, and D. L. Huffaker, Nanotechnology **24**, 475601 (2013).
[16]K. Shimamura, Z. S. Yuan, F. Shimojo, and A. Nakano, Appl. Phys. Lett. **103**(2), 022105 (2013).
[17]C. Thelander, P. Caroff, S. Plissard, A. W. Dey, and K. A. Dick, Nano Lett. **11**(6), 2424–2429 (2011).
[18]S. Cahangirov and S. Ciraci, Phys. Rev. B **79**, 165118 (2009).
[19]M. Rosini and R. Magri, ACS Nano **4**(10), 6021–6031 (2010).
[20]V. Pankoke, P. Kratzer, and S. Sakong, Phys. Rev. B **84**, 075455 (2011).
[21]C. J. Sandroff, R. N. Nottenburg, J. C. Bischoff, and R. Bhat, Appl. Phys. Lett. **51**(1), 33–35 (1987).
[22]K. N. Ow and X. W. Wang, Phys. Rev. B **54**(24), 17661–17666 (1996).
[23]T. H. Yu, L. Yan, W. You, R. B. Laghumavarapu, D. L. Huffaker, and C. Ratsch, Appl. Phys. Lett. **103**, 173902 (2013).
[24]W. C. Wang, G. Lee, M. Huang, R. M. Wallace, and K. J. Cho, J. Appl. Phys. **107**(10), 103720 (2010).
[25]H. Oigawa, J. F. Fan, Y. Nannichi, K. Ando, K. Saiki, and A. Koma, Jpn. J. Appl. Phys., Part 2 **28**(3), L340–L342 (1989).
[26]H. Ohno, H. Kawanishi, Y. Akagi, Y. Nakajima, and T. Hijikata, Jpn. J. Appl. Phys., Part 1 **29**(11), 2473–2476 (1990).
[27]V. Blum, R. Gehrke, F. Hanke, P. Havu, V. Havu, X. G. Ren, K. Reuter, and M. Scheffler, Comput. Phys. Commun. **180**(11), 2175–2196 (2009).
[28]J. P. Perdew, K. Burke, and M. Ernzerhof, Phys. Rev. Lett. **77**(18), 3865–3868 (1996).
[29]A. Tkatchenko and M. Scheffler, Phys. Rev. Lett. **102**(7), 073005 (2009).